Eur. Phys. J. B **5**, 317–324 (1998)

THE EUROPEAN PHYSICAL JOURNAL B

Effective Hamiltonians for holes in antiferromagnets: a new approach to implement forbidden double occupancy*

W. Apel[1], H.-U. Everts[2], and U. Körner[2,a]

[1] Physikalisch-Technische Bundesanstalt, Bundesallee 100, 38116 Braunschweig, Germany
[2] Institut für Theoretische Physik, Universität Hannover, Appelstrasse 2, 30167 Hannover, Germany

Received: 23 December 1997 / Accepted: 17 March 1998

Abstract. A coherent state representation for the electrons of ordered antiferromagnets is used to derive effective Hamiltonians for the dynamics of holes in such systems. By an appropriate choice of these states, the constraint of forbidden double occupancy can be implemented rigorously. Using these coherent states, one arrives at a path integral representation of the partition function of the systems, from which the effective Hamiltonians can be read off. We apply this method to the $t-J$ model on the square lattice and on the triangular lattice. In the former case, we reproduce the well-known fermion-boson Hamiltonian for a hole in a collinear antiferromagnet. We demonstrate that our method also works for non-collinear antiferromagnets by calculating the spectrum of a hole in the triangular antiferromagnet in the self-consistent Born approximation and by comparing it with numerically exact results.

PACS. 75.10.Jm Quantized spin models – 71.10.Fd Lattice fermion models – 75.50.Ee Antiferromagnetics

1 Introduction

It is widely recognized that an accurate description of the dynamics of holes in antiferromagnetically (AF) ordered materials is an important first step towards an understanding of the essential physics of the cuprate superconductors. Consequently, numerous investigations [1–13] have dealt with the problem of a single hole in a square-lattice antiferromagnet. Most of these studies are based on an effective Hamiltonian $\mathcal{H}_\Box$ [14,15] which describes the hole as a spinless fermion which is coupled to bosons representing the collective excitations (magnons) of the antiferromagnetic background. The structure of this effective Hamiltonian reflects the two-sublattice structure of the square lattice AF. When the hole hops between nearest neighbour lattice sites, it necessarily disturbs the magnetic order. Thus, any move of the hole requires absorption or emission of a magnon. Derivations of $\mathcal{H}_\Box$ from the $t-J$ Hamiltonian have revealed the approximate nature of this effective Hamiltonian [16], and to obtain the spectrum of a hole from $\mathcal{H}_\Box$ further approximations are necessary. Most often, the fermion-magnon coupling is treated in the self-consistent Born approximation (SCBA) which was already used in the original studies by Kane *et al.* [14] and Marsiglio *et al.* [15]. Surprisingly, the approximate spectra obtained in this manner agree excellently with the spectra of small clusters obtained by numerically exact diagonalization of the $t-J$ Hamiltonian for these clusters.

Apart from its relevance to the physics of cuprate superconductors, the dynamics of holes in ordered antiferromagnets is a highly nontrivial problem of the physics of strongly correlated electron systems, and it is therefore of fundamental theoretical interest. Here, we shall present a derivation of effective Hamiltonians for holes in AFs which is not restricted to any particular type of magnetic order. Our method does not provide us with a unique effective Hamiltonian for an arbitrary number of holes. Rather the cases of a single hole, two holes and in general an arbitrary but fixed number of holes have to be treated separately. While our presentation remains general, we shall confine ourselves to the single-hole problem in order to demonstrate our method's practical applicability. In particular, we shall derive and evaluate the effective Hamiltonian $\mathcal{H}_\triangle$ for a single hole in the triangular AF.

2 Effective Lagrangian

For definiteness, we consider the $t-J$ Hamiltonian,

$$\mathcal{H} = -t \sum_{\substack{\langle \mathbf{r},\mathbf{r}' \rangle \\ \sigma}} \hat{P}(c^\dagger_{\mathbf{r},\sigma} c_{\mathbf{r}',\sigma} + h.c.)\hat{P} + J \sum_{\langle \mathbf{r},\mathbf{r}' \rangle} \hat{\mathbf{S}}_\mathbf{r} \cdot \hat{\mathbf{S}}_{\mathbf{r}'} \,. \quad (1)$$

t and J are the single particle hopping matrix element and the exchange constant, respectively, the operator $\hat{P}$ projects onto states in which each of the N_s lattice sites

* Dedicated to J. Zittartz on the occasion of his 60th birthday
[a] e-mail: koerner@itp.uni-hannover.de

is either empty or singly occupied, and $\hat{\mathbf{S}}_{\mathbf{r}} = \frac{1}{2} c^{\dagger}_{\mathbf{r},\alpha} \boldsymbol{\sigma}_{\alpha,\beta} c_{\mathbf{r},\beta}$ is the electron spin expressed in terms of creation and annihilation operators, $c^{\dagger}_{\mathbf{r},\alpha}$ and $c_{\mathbf{r},\alpha}$, for fermion states at site $\mathbf{r}$ with spin projection α. The sums in (1) run over pairs $\langle\ ,\ \rangle$ of nearest neighbour sites of the lattice.

In order to cast the partition function $\mathcal{Z} = \mathrm{tr}[\exp\{-\beta\mathcal{H}\}]$ into the form of a path integral, we introduce the following coherent states [13] for each lattice site $\mathbf{r}$ (we omit the site index wherever this does not lead to ambiguities):

$$
\begin{aligned}
|\omega\rangle &= e^{\left[\eta c - c^{\dagger}\eta^{*}\right]} |\Omega\rangle, \\
|\Omega\rangle &= c^{\dagger}|0\rangle, \\
c^{\dagger} &= e^{-i\phi/2}\cos\frac{\theta}{2} e^{-i\psi/2} c^{\dagger}_{\uparrow} + e^{i\phi/2}\sin\frac{\theta}{2} e^{-i\psi/2} c^{\dagger}_{\downarrow}. \quad (2)
\end{aligned}
$$

Here, η, η^{*} are Grassmann variables, and $|0\rangle$ is the vacuum with no spins present. Obviously, $|\Omega\rangle$ is a one-fermion state with spin in the direction (θ, ϕ) on the sphere. The inclusion of a phase factor which depends on the third Euler angle ψ is necessary, if $|\Omega\rangle$ and η are to satisfy the following requirements: (i) $|\Omega\rangle$ is to transform covariantly under *all* $SU(2)$ operations, while (ii) η remains invariant under these operations. As will be seen shortly, both requirements appear natural in view of the physical interpretation of the variables $\Omega = (\psi, \theta, \phi)$ and η. It is easily checked that the states $|\omega\rangle$ *include* the empty and the spin-up and spin-down states of the fermion, but *exclude* the doubly occupied state. In fact, the states $|\omega\rangle$ are complete in this three-dimensional space,

$$
\begin{aligned}
&\int d\omega\, |\omega\rangle\langle\omega| := \int d\Omega\, \frac{1}{2} \int d\eta^{*} d\eta\, e^{-\eta^{*}\eta} |\omega\rangle\langle\omega| \\
&= \int d\Omega\, \frac{1}{2} \int d\eta^{*} d\eta\, e^{-2\eta^{*}\eta} \left\{ \eta\, \eta^{*} |0\rangle\langle 0| + |\Omega\rangle\langle\Omega| \right\} \\
&= \mathbf{1}_3 \qquad (3)
\end{aligned}
$$

where $\int d\Omega \cdots = \frac{1}{8\pi^2} \int_0^{4\pi} d\psi \int_0^{\pi} d\theta \sin\theta \int_0^{2\pi} d\phi\ \ldots$ The Euler angles Ω describe the spin degrees of freedom and the Grassmann variables η and η^{*} a spinless fermionic hole. Thus the requirement (ii) is cogent. With these coherent states, the standard steps towards a path integral representation of the partition function yield

$$
\begin{aligned}
\mathcal{Z}_M = \int \mathcal{D}_M[\Omega] \int \mathcal{D}_M[\eta^{*}, \eta] \\
\times \prod_{\substack{\tau=1 \\ \mathbf{r}}}^{M} \left(\langle \Omega_{\tau-1,\mathbf{r}} | \Omega_{\tau,\mathbf{r}} \rangle \frac{1}{2} e^{-2\eta^{*}_{\tau,\mathbf{r}}\eta_{\tau,\mathbf{r}}} \right) \\
\times \exp\left\{ \sum_{\tau,\mathbf{r}} \frac{\eta^{*}_{\tau-1,\mathbf{r}}\eta_{\tau,\mathbf{r}}}{\langle \Omega_{\tau-1,\mathbf{r}} | \Omega_{\tau,\mathbf{r}} \rangle} \right. \\
\left. + \sum_{\tau} \ln\left[1 + \frac{\langle \omega_{\tau-1} | e^{-\Delta\tau\mathcal{H}} - 1 | \omega_{\tau} \rangle}{\langle \omega_{\tau-1} | \omega_{\tau} \rangle} \right] \right\}, \quad (4)
\end{aligned}
$$

with $\mathcal{D}_M[\Omega] = \prod_{\tau=1,\mathbf{r}}^{M} d\Omega_{\tau,\mathbf{r}}$ and $\mathcal{D}_M[\eta^{*}, \eta] = \prod_{\tau=1,\mathbf{r}}^{M} d\eta^{*}_{\tau,\mathbf{r}}\, d\eta_{\tau,\mathbf{r}}$. Here, sums and products run over the M (imaginary) time slices of the Trotter decomposition of $\exp(-\beta\mathcal{H})$ (subscript τ) and over the N_s lattice sites (subscript $\mathbf{r}$). $\Delta\tau = \beta/M$ is the width of the time slices. The boundary conditions are $\Omega_{0,\mathbf{r}} = \Omega_{M,\mathbf{r}}$ and $\eta^{(*)}_{0,\mathbf{r}} = -\eta^{(*)}_{M,\mathbf{r}}$. The final step in the conversion of $\mathcal{Z}_M$ into a path integral would be to take the continuum limit $M \to \infty$ in the time direction. This meets with difficulties. After the expansion of the second exponential in (4) to linear order in $\Delta\tau$, a factor $\prod_{\tau,\mathbf{r}} e^{-\eta^{*}_{\tau,\mathbf{r}}\eta_{\tau,\mathbf{r}}}$ remains in the integrand which is therefore *ill* defined in the limit $M \to \infty$. However, as we shall show now, the individual summands $\mathcal{Z}^{n-hole}$ in the decomposition

$$
\mathcal{Z}_M = \mathcal{Z}_M^{0-hole} + \mathcal{Z}_M^{1-hole} + \ldots + \mathcal{Z}_M^{n-hole} + \ldots \qquad (5)
$$

of the partition function $\mathcal{Z}_M$ into $0-$, $1-$, $\ldots n-$hole contributions are *well*-defined in the τ-continuum limit. Since in this work we are interested in the one-hole effective Hamiltonian, which can be extracted from $\mathcal{Z}^{1-hole}$, we confine our attention to the first two terms of (5). The crucial elements in this decomposition are the weight factors $e^{-2\eta^{*}_{\tau,\mathbf{r}}\eta_{\tau,\mathbf{r}}} = 1 - 2\eta^{*}_{\tau,\mathbf{r}}\eta_{\tau,\mathbf{r}}$ in the integrand of (4). From (3) it follows that the identity in such a factor projects onto configurations with a hole at $(\tau, \mathbf{r})$ while the second term, $-2\,\eta^{*}_{\tau,\mathbf{r}}\eta_{\tau,\mathbf{r}}$, projects onto configurations with an electron at $(\tau, \mathbf{r})$. Thus, by retaining in the integrand of (4) only the term $\prod_{\tau,\mathbf{r}} \left(-2\eta^{*}_{\tau,\mathbf{r}}\eta_{\tau,\mathbf{r}}\right)$ of the expansion of $\prod_{\tau,\mathbf{r}} \left(1 - 2\eta^{*}_{\tau,\mathbf{r}}\eta_{\tau,\mathbf{r}}\right)$, one obtains $\mathcal{Z}^{0-hole}$, the partition function with no hole at all which is, of course, the partition function of the Heisenberg Hamiltonian. Similarly, by retaining those terms of the expansion which contain for each time slice τ just $N_s - 1$ factors $-2\eta^{*}_{\tau,\mathbf{r}}\eta_{\tau,\mathbf{r}}$ one obtains $\mathcal{Z}_M^{1-hole}$. (The number of holes remains constant in time.) Using the identity

$$
\prod_{\tau,\mathbf{r}} \left(\frac{1}{2} e^{-2\eta^{*}_{\tau,\mathbf{r}}\eta_{\tau,\mathbf{r}}} \right) \Big|_{1-hole} = \frac{1}{2^M} \prod_{\tau,\mathbf{r}} \left(e^{-\eta^{*}_{\tau,\mathbf{r}}\eta_{\tau,\mathbf{r}}} \right) \Big|_{1-hole}, \qquad (6)
$$

which holds between the one-hole projectors on both sides, we can now cast $\mathcal{Z}_M^{1-hole}$ into the form

$$
\begin{aligned}
\mathcal{Z}_M^{1-hole} = \frac{1}{2^M} \int \mathcal{D}_M[\Omega] \int \mathcal{D}_M[\eta^{*}, \eta] \\
\times \prod_{\substack{\tau=1 \\ \mathbf{r}}}^{M} \left(\langle \Omega_{\tau-1,\mathbf{r}} | \Omega_{\tau,\mathbf{r}} \rangle \right) \\
\times \exp\left\{ - \sum_{\tau,\mathbf{r}} \left(\eta^{*}_{\tau,\mathbf{r}}\eta_{\tau,\mathbf{r}} - \frac{\eta^{*}_{\tau-1,\mathbf{r}}\eta_{\tau,\mathbf{r}}}{\langle \Omega_{\tau-1,\mathbf{r}} | \Omega_{\tau,\mathbf{r}} \rangle} \right) \right. \\
\left. + \sum_{\tau} \ln\left[1 + \frac{\langle \omega_{\tau-1} | e^{-\Delta\tau\mathcal{H}} - 1 | \omega_{\tau} \rangle}{\langle \omega_{\tau-1} | \omega_{\tau} \rangle} \right] \right\} \Big|_{1-hole}. \qquad (7)
\end{aligned}
$$

The additional factor of $1/2$ associated with each time slice τ finds a natural explanation: It compensates for the integrations over the redundant spin variable at the position of the hole [17]. Obviously, the integrand of (7) is well

defined in the τ-continuum limit $M \to \infty$. Performing this limit, one obtains

$$\mathcal{Z}^{1-hole} = \int \mathcal{D}[\Omega] \int \mathcal{D}[\eta^*, \eta]\ e^{\int_0^\beta d\tau \mathcal{L}} \Big|_{1-hole} \tag{8}$$

with the classical Lagrangian for one hole

$$\mathcal{L} = \sum_{\mathbf{r}} \left[1 - \eta^*_{\mathbf{r}}(\tau)\eta_{\mathbf{r}}(\tau)\right] \langle \Omega_{\mathbf{r}}(\tau)|\dot{\Omega}_{\mathbf{r}}(\tau)\rangle + \sum_{\mathbf{r}} \eta^*_{\mathbf{r}}(\tau)\dot{\eta}_{\mathbf{r}}(\tau) - \langle \omega(\tau)|\mathcal{H}|\omega(\tau)\rangle_{1-hole}. \tag{9}$$

Here, $|\omega(\tau)\rangle = \prod_{\mathbf{r}} |\omega_{\mathbf{r}}(\tau)\rangle$, and $\langle \omega(\tau)|\mathcal{H}|\omega(\tau)\rangle_{1-hole}$ denotes that part of the expectation value which is bilinear in the Grassmann fields η^*, η.

It should be clear from these considerations that in order to determine the effective interaction between a pair of holes, one will have to analyze the 2-hole contribution to $\mathcal{Z}_M$. In calculating it from the 1-hole contribution by integrating over the spin degrees of freedom, one would miss a part of this interaction.

Evaluating (9) with the states (2) and the Hamiltonian (1) of the $t-J$ model on an arbitrary lattice, we obtain $\mathcal{L} = \mathcal{L}_{kin} + \mathcal{L}_t + \mathcal{L}_J$, where (we omit total time derivatives)

$$\mathcal{L}_{kin} = \sum_{\mathbf{r}} \left[\eta^*_{\mathbf{r}}\dot{\eta}_{\mathbf{r}} + \frac{i}{2}\eta^*_{\mathbf{r}}\eta_{\mathbf{r}}\dot{\psi}_{\mathbf{r}} - \frac{i}{2}\left(1 - \eta^*_{\mathbf{r}}\eta_{\mathbf{r}}\right)\dot{\phi}_{\mathbf{r}}\cos(\theta_{\mathbf{r}}) \right], \tag{10}$$

$$\mathcal{L}_t = -t \sum_{\langle \mathbf{r},\mathbf{r}'\rangle} \Big\{ \eta^*_{\mathbf{r}'}\eta_{\mathbf{r}} e^{-\frac{i}{2}(\psi_{\mathbf{r}'} - \psi_{\mathbf{r}})} \times \left[\cos\left(\frac{\phi_{\mathbf{r}} - \phi_{\mathbf{r}'}}{2}\right)\cos\left(\frac{\theta_{\mathbf{r}} - \theta_{\mathbf{r}'}}{2}\right) + i\sin\left(\frac{\phi_{\mathbf{r}} - \phi_{\mathbf{r}'}}{2}\right)\cos\left(\frac{\theta_{\mathbf{r}} + \theta_{\mathbf{r}'}}{2}\right) \right] + (\mathbf{r} \leftrightarrow \mathbf{r}') \Big\} \tag{11}$$

and

$$\mathcal{L}_J = -J \sum_{\langle \mathbf{r},\mathbf{r}'\rangle} \left(1 - \eta^*_{\mathbf{r}}\eta_{\mathbf{r}} - \eta^*_{\mathbf{r}'}\eta_{\mathbf{r}'}\right) \mathbf{S}_{\mathbf{r}} \cdot \mathbf{S}_{\mathbf{r}'}\ . \tag{12}$$

The Heisenberg term $\mathcal{L}_J$ accounts for the interaction between spins $\mathbf{S} = \frac{1}{2}(\sin\theta\cos\phi, \sin\theta\sin\phi, \cos\theta)$ at sites where no hole is present. $\mathcal{L}_t$ describes the hopping of the hole; the hopping energy depends on the state of the spins. Finally, $\mathcal{L}_{kin}$ contains the kinetic terms of a spinless hole ($\eta^*\dot{\eta}$), and a spin 1/2, *i.e.* $\dot{\phi}\cos(\theta)$. In addition, two terms couple the hole to the angular degrees of freedom. The second cancels the kinetic term of the spin at sites where a hole is present. The first has the form of a gauge interaction with the field ψ. It is tempting to use a parameterization in which the factor $\exp(\frac{i}{2}\psi)$ is absorbed in η, since then, all the ψ dependent terms in $\mathcal{L}$ disappear. However, after such a gauge transformation, η is no longer invariant under $SU(2)$ operations, as explained above in connection with the choice of the coherent states (2). Since this has unwanted consequences, we do not follow this route.

In summary, our procedure for obtaining effective Hamiltonians consists of the following steps: first we represent the partition function of the initial quantum Hamiltonian as a discrete-time path integral; then, we identify that part of the partition function that corresponds to the number of holes we wish to consider; in this part, we then perform the continuum limit to obtain the classical Lagrangian; finally, we translate back to an effective quantum Hamiltonian.

The Lagrangian $\mathcal{L}$, (10-12), still represents the full nonlinear problem of a hole interacting with the spin background. In the following, we shall confine ourselves to a spin wave expansion around the classical spin groundstate of $\mathcal{L}$. In this picture, the hole moves in a spin background described by angular fields which deviate little from their groundstate. The spin wave expansions have, of course, to be performed separately for the case of collinear spin order (square lattice AF) and for the case of planar spin order (triangular lattice AF). We shall briefly rederive the quantum Hamiltonian, $\mathcal{H}_\square$, which is well known for the case of collinear spin order. For the case of planar spin order, we obtain a significantly different effective Hamiltonian $\mathcal{H}_\triangle$. To check the validity of the approximations that lead to $\mathcal{H}_\triangle$ we shall calculate the one hole spectral properties that follow from $\mathcal{H}_\triangle$ and compare them with results obtained by numerically exact diagonalization of the $t-J$ model for small finite lattice cells.

3 One hole on a square lattice

The two sublattice classical AF order is reproduced by assigning the value $\pi/2$ to $\theta_{\mathbf{r}}$ and the values $\phi^{(0)}_{\mathbf{r}} = \pm\pi/2$ to $\phi_{\mathbf{r}}$ for $\mathbf{r}$ from the A or B lattice, respectively. The deviations from the ordered groundstate, $x_{\mathbf{r}}$ and $p_{\mathbf{r}}$ defined by

$$\phi_{\mathbf{r}} = \phi^{(0)}_{\mathbf{r}} + \sqrt{2}x_{\mathbf{r}} \qquad \theta_{\mathbf{r}} = \frac{\pi}{2} + \sqrt{2}p_{\mathbf{r}}\ , \tag{13}$$

are canonically conjugate harmonic oscillator fields as can be seen from $\mathcal{L}_{kin}$. Now, we expand $\mathcal{L}$ up to quadratic order in the amplitudes $a = (x - ip)/\sqrt{2}$ and a^* and keep in the quadratic term only the leading zero-hole contribution. Then, the spin and the hole degrees of freedom decouple in $\mathcal{L}_{kin}$. We redefine the hole field by $h \equiv \eta\, e^{\frac{i}{2}(\psi - \phi^{(0)})}$. Then, all the phases in the hopping term in the path integral become equal; the field ψ disappears from $\mathcal{L}$ and is integrated out. Finally, we translate back to operator form and get

$$\mathcal{H}_\square = -t \sum_{\langle \mathbf{r},\mathbf{r}'\rangle} \left[h^\dagger_{\mathbf{r}'} h_{\mathbf{r}}\, i\, \left(a^\dagger_{\mathbf{r}} - a_{\mathbf{r}'}\right) + h.c. \right] + \frac{J}{2} \sum_{\langle \mathbf{r},\mathbf{r}'\rangle} \left(a^\dagger_{\mathbf{r}} a_{\mathbf{r}} + a^\dagger_{\mathbf{r}'} a_{\mathbf{r}'} - a^\dagger_{\mathbf{r}} a^\dagger_{\mathbf{r}'} - a_{\mathbf{r}'} a_{\mathbf{r}} \right) + J \sum_{\mathbf{r}} \left(h^\dagger_{\mathbf{r}} h_{\mathbf{r}} - \frac{1}{2} \right). \tag{14}$$

$\mathcal{H}_\square$ is, up to a canonical transformation ($a_{\mathbf{r}} \to -ia_{\mathbf{r}}$) identical with the Hamiltonian considered in [15]. The last term in $\mathcal{H}_\square$, containing the hole number, accounts for the breaking of four bonds per hole in the classical groundstate.

4 One hole in the triangular lattice

In the classical limit, the groundstate of the $t-J$ model at half filling is the well-known planar 120° spin structure: $\theta_{\mathbf{r}}^{(0)} = \pi/2$ for all $\mathbf{r}$ and $\phi_{\mathbf{r}}^{(0)} = 2\pi/3, 0, -2\pi/3$ for the A, B and C sublattice, respectively. As in the case of the square lattice, we describe the deviations from this ordered groundstate by the spin wave amplitudes $x_{\mathbf{r}}$ and $p_{\mathbf{r}}$ which are canonically conjugate harmonic oscillator fields.

Proceeding as in the square lattice case, *i.e.* expanding to second order in the amplitudes a and a^* and integrating over ψ, one would be left with terms in $\mathcal{L}_t$ that couple the hole motion to zero energy spin modes. But these modes are uniform spin rotations which are exact symmetries of the initial model (1). Therefore, they cannot appear in any order of a perturbation expansion. In the Appendix, we trace this apparent inconsistency back to the integration over the field ψ. We show how to derive a result which is free of zero modes, as it should be, and we explain why the same difficulty does not occur in the case of the square lattice. Retaining terms of the same order in the amplitudes a, a^* as in the square lattice case, we find the following effective Hamiltonian for one hole in the triangular AF (in momentum space)

$$\begin{aligned}\mathcal{H}_{\triangle} = & \frac{3J}{4}\sum_{\mathbf{q}}\left\{(2+w_{\mathbf{q}})a_{\mathbf{q}}^{\dagger}a_{\mathbf{q}} - \frac{3w_{\mathbf{q}}}{2}(a_{-\mathbf{q}}^{\dagger}a_{\mathbf{q}}^{\dagger} + a_{-\mathbf{q}}a_{\mathbf{q}})\right\} \\ & -\frac{3JN_s}{8} + \sum_{\mathbf{q}}\epsilon_{\mathbf{q}}\, h_{\mathbf{q}}^{\dagger}h_{\mathbf{q}} \\ & +\frac{1}{\sqrt{N_s}}\sum_{\mathbf{q},\mathbf{q}'}\left\{f_{\mathbf{q},\mathbf{q}'}\, h_{\mathbf{q}}^{\dagger}h_{\mathbf{q}'}\, a_{\mathbf{q}-\mathbf{q}'} + h.c.\right\}\ . \end{aligned} \tag{15}$$

The terms in the first line are nothing but the linear spin wave approximation (LSW) of the triangular Heisenberg AF. The last line contains the coupling between the hole and the magnons with the hole-magnon vertex

$$\begin{aligned} f_{\mathbf{q},\mathbf{q}'} = & 3\sqrt{3}i\left[-t\gamma_{\mathbf{q}'} + \frac{J}{4}\gamma_{\mathbf{q}-\mathbf{q}'}\right] \\ & +\sqrt{3}\left(\frac{1}{2} + w_{\mathbf{q}-\mathbf{q}'} - i\gamma_{\mathbf{q}-\mathbf{q}'}\right) \\ & \times\left[t(w_{\mathbf{q}} - w_{\mathbf{q}'}) + \frac{J}{2}(1 - w_{\mathbf{q}-\mathbf{q}'})\right]\ . \end{aligned} \tag{16}$$

Here, $w_{\mathbf{q}}$ is defined by

$$w_{\mathbf{q}} + i\gamma_{\mathbf{q}} = \frac{1}{3}\sum_{j=1}^{3} e^{i\mathbf{q}\cdot\boldsymbol{\delta}_j} \tag{17}$$

and $\boldsymbol{\delta}_j = (\cos\varphi_j, \sin\varphi_j)$, $\varphi_j = ((2\pi/3)j)$, are the vectors to three of the six nearest neighbour sites on the triangular lattice. As opposed to the square lattice, the hole can hop on the triangular lattice without emission or absorption of a magnon. This is expressed by the second line of (15) where

$$\epsilon_{\mathbf{q}} = \frac{3J}{4} - 3tw_{\mathbf{q}}\ , \tag{18}$$

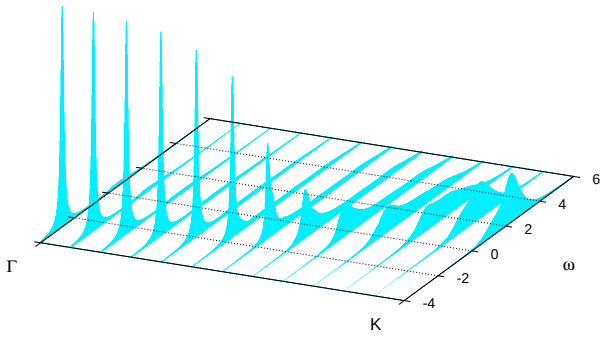

Fig. 1. Spectral density $A(\mathbf{k},\omega)$ in SCBA approximation for $N_s = 36\times 36$ sites, $t = J = 1$, and for $\mathbf{k}$ values taken along a straight line from Γ to K (*cf.* Fig. 2) ($\eta = 0.1$).

is just half the dispersion of a particle hopping between nearest neighbour sites of the empty triangular lattice. $\mathcal{H}_{\triangle}$ constitutes our main result for the Hamiltonian of one hole in the $t-J$ model on a triangular lattice in spin wave approximation [20]. In the following, we analyze its content by treating the hole magnon coupling in the simplest approximation.

4.1 Born approximation of the selfenergy

Following previous treatments of the square lattice case [15], we employ the SCBA to obtain the selfenergy $\Sigma(\mathbf{k},\omega)$ of one hole. We denote the Green's function of one hole by $G(\mathbf{k},\omega) = (\omega - \epsilon_{\mathbf{k}} - \Sigma(\mathbf{k},\omega))^{-1}$. Then,

$$\begin{aligned}\Sigma^{SCBA}(\mathbf{k},\omega) = & \frac{1}{N_s}\sum_{\mathbf{k}'}\left|u_{\mathbf{k}-\mathbf{k}'}f_{\mathbf{k},\mathbf{k}'} + v_{\mathbf{k}-\mathbf{k}'}f_{\mathbf{k}',\mathbf{k}}^{*}\right|^2 \\ & \times G^{SCBA}(\mathbf{k}', \omega - \omega_{\mathbf{k}-\mathbf{k}'})\ . \end{aligned} \tag{19}$$

Here, $\omega_{\mathbf{q}} = \frac{3J}{2}\sqrt{(1+2w_{\mathbf{q}})(1-w_{\mathbf{q}})}$ is the spin wave energy. $u_{\mathbf{q}}$ and $v_{\mathbf{q}}$ are the Bogoliubov amplitudes,

$$\begin{aligned} u_{\mathbf{q}} &= \left\{\frac{1}{2}\left[\frac{3J(1+w_{\mathbf{q}}/2)}{2\omega_{\mathbf{q}}} + 1\right]\right\}^{1/2} \\ v_{\mathbf{q}} &= \mathrm{sgn}(w_{\mathbf{q}})\left\{\frac{1}{2}\left[\frac{3J(1+w_{\mathbf{q}}/2)}{2\omega_{\mathbf{q}}} - 1\right]\right\}^{1/2}. \end{aligned}$$

From the Green's function, the spectral density is obtained as $A(\mathbf{k},\omega) = -\frac{1}{\pi}\lim_{\eta\to 0^+}\mathrm{Im}\, G(\mathbf{k},\omega+i\eta)$. The parameter η regularizes the spectral density[1]. Equation (19) has been solved by numerical iteration starting with $\Sigma = 0$ for a lattice of $N_s = 36\times 36$ sites with periodic boundary conditions. In Figure 1 we display for $t = 1$, $J = 1$ the spectral density $A(\mathbf{k},\omega)$ on $\mathbf{k}$–points along a straight

[1] For $N_s = 24$ the crystal momentum of the one hole groundstate is an interior point close to K of the Brillouin zone. This is the reason, why for $N_s = 24$ the values of δE_1^{ex} deviate significantly from the rest.

Table 1. Exact and approximate groundstate energies of samples of N_s sites of the $t-J$ model with $n_h(=0,1)$ holes. E_0: groundstate energies in the half filled case. $E_{1,loc}$: energies for creating a localized hole. δE_1: energy gain of the hole due to delocalization.

	exact diagonalization				linear spin wave, SCBA			
	$t=0$		$t=0.1$	$t=1$	$t=0$		$t=0.1$	$t=1$
N_s	$n_h=0$ E_0^{ex}	$n_h=1$ $E_{1,loc}^{ex}$	$n_h=1$ δE_1^{ex}	$n_h=1$ δE_1^{ex}	$n_h=0$ E_0^{LSW}	$n_h=1$ $E_{1,loc}^{SCBA}$	$n_h=1$ δE_1^{SCBA}	$n_h=1$ δE_1^{SCBA}
9	−5.25000	0.50000	0.40000	4.00000	−5.62500	0.66884	0.31627	3.18974
12	−7.32396	1.15197	0.38544	4.09035	−7.25658	0.64520	0.32854	3.39377
21	−11.78091	0.56862	0.39986	4.06326	−11.82919	0.65145	0.32504	3.35476
24[1]	−12.93870	0.92897	0.29581	3.42937	−13.04174	0.65227	0.32561	3.36573
27	−15.12597	0.59201	0.38805	3.99864	−15.04634	0.65052	0.32572	3.36510

line from the centre Γ to the corner K of the Brillouin zone (*cf.* Fig. 2). The main feature of the spectra is a pronounced quasiparticle peak. For $t=0$, the quasiparticle dispersion is flat throughout the Brillouin zone. For increasing t, a dispersion with the minimum at Γ emerges and the peak broadens. Around Γ, the quasiparticle peak persists for values of t up to $10J$; near K it already decays for $t > 0.2J$.

4.2 Comparison with exact numerical diagonalization results

As we have pointed out in the course of the derivation, the effective Hamiltonian $\mathcal{H}_\Delta$ is an approximate result, and the computation of the one-hole Green's function is based on the self-consistent Born approximation. In order to have a check on the validity of these approximations, we computed the spectral density $A(\mathbf{k},\omega)$ and related quantities directly for the $t-J$ model on small periodic samples of the triangular lattice with N_s sites. Numerically exact results for the quantities in question were obtained by applying the Lanczos technique (see *e.g.* [1]) to the Hamiltonian of these samples. In these computations, the exchange constant J has been set equal to unity throughout. Results for the groundstate energies for half filling ($n_h=0$) and for one hole ($n_h=1$) are displayed in Table 1 together with the approximate LSW and SCBA energies for the same sample sizes. For $t\neq 0$, the groundstate wave function of the hole is an extended state with crystal momentum at the high symmetry points of the Brillouin zone; Γ for odd N_s and K for even N_s.

For the half filled case, the $t-J$ Hamiltonian reduces to the Heisenberg Hamiltonian, and it is well known that in this case the LSW results E_0^{LSW} are in good agreement with the exact results E_0^{ex}, in particular for the larger system sizes [18]. Turning to the one-hole results, we first discuss the case $t=0$ in which the hole is localized. $E_{1,loc}$ is the energy needed to create a localized hole in the half filled groundstate. There is a strong even-odd staggering in the exact results (2nd column of Tab. 1): in the even samples (N_s even) in which the spins pair up to a singlet, $S_{tot}=0$, the "binding energy" per electron is larger than

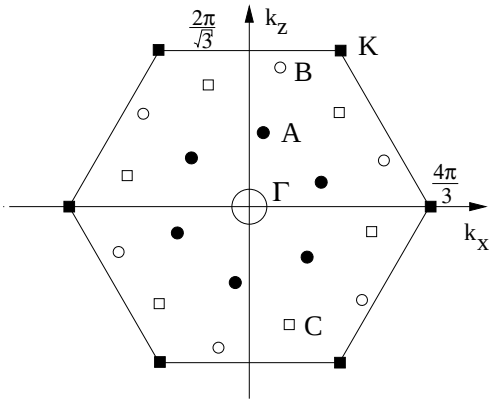

Fig. 2. The Brillouin zone of the $N_s=21$ system shows a sixfold symmetry.

in the odd systems which contain an unsaturated spin, $S_{tot}=1/2$. This is a finite size effect which, as is seen in Table 1, decreases very slowly with the sample size. Nevertheless, the exact values $E_{1,loc}^{ex}$ appear to converge to the SCBA value $E_{1,loc}^{SCBA}$ in an alternating fashion. That the even-odd staggering is absent from $E_{1,loc}^{SCBA}$ is understandable, since the SCBA is based on the spin wave spectrum of the infinite sample.

For finite hopping amplitude $t\neq 0$, the hole becomes delocalized. It is suggestive to write the hole energy as $E_1 = E_{1,loc} - \delta E_1(t)$, where $\delta E_1(t)$ is the energy gain due to delocalization of the hole wave function. The results in Table 1 show that δE_1 increases linearly with t, $\delta E_1(t) = \alpha t$. This assertion has been verified by computing $\delta E_1(t)$ for a sequence of values $0.1 < t < 1$ not shown in Table 1. The coefficient α is seen to differ significantly between the exact results and the SCBA, $\alpha^{ex}\approx 4$, $\alpha^{SCBA}\approx 3.36$. At present, we are not in a position to decide whether this discrepancy is inherent in the effective Hamiltonian $\mathcal{H}_\triangle$ or whether it is a deficiency of the SCBA.

Next we compare the exact and the SCBA results for the spectral density $A(\mathbf{k},\omega)$. Figure 3 shows the spectral density of one hole in the $N_s=21$ sample at the centre (Γ) and at the corner (K) of the Brillouin zone (*cf.* Fig. 2) for the parameter values $J=1$ and $t=0.1$, $t=1$. The solid

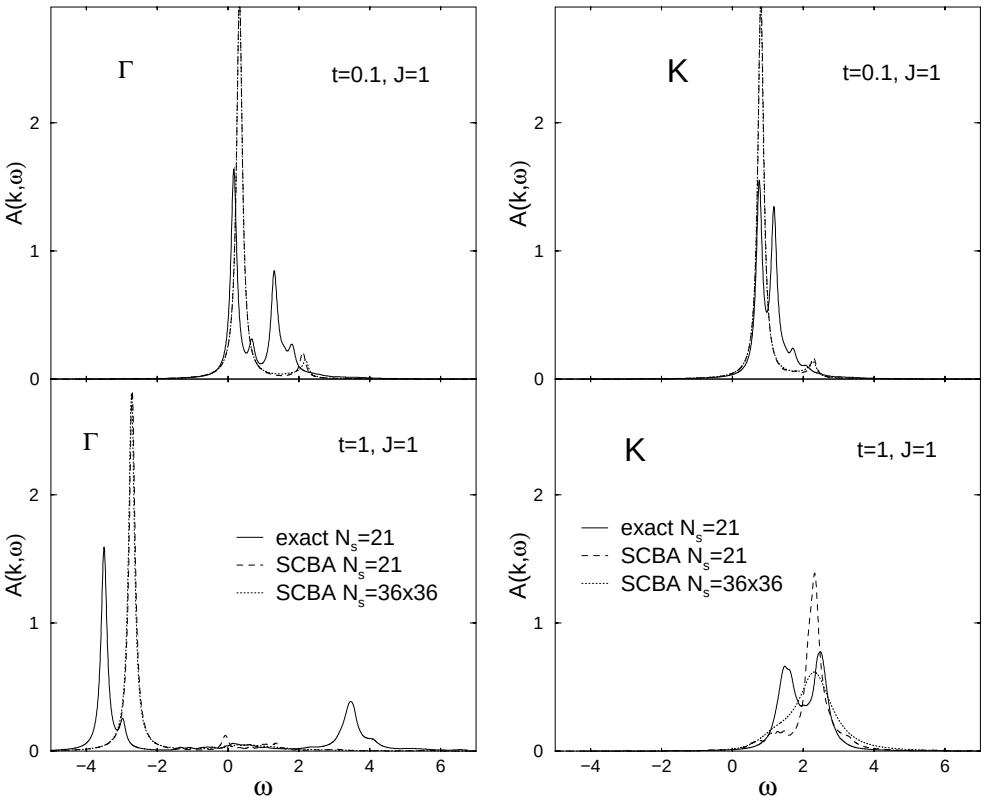

Fig. 3. Spectral density (a) at the Γ point and (b) at the corner K of the Brillouin zone for $t = 0.1$ and $t = 1$ for $J = 1$. The solid line shows the exact results for the $N_s = 21$ sites, the dashed (dotted) line the result of the SCBA for $N_s = 21$ ($N_s = 36 \times 36$) sites. ω is measured against E_0^{ex} and E_0^{LSW} ($\eta = 0.1$).

lines are the results of the exact diagonalization which were obtained from a continued fraction expansion [19] of the Lanczos results. The dashed lines are the result of the SCBA for $N_s = 21$. For $t = 0.1$ there is a well defined quasiparticle peak in the exact results at the bottom of the spectrum. This peak is nicely reproduced by the SCBA.

For $t = 1$, a quasiparticle peak is still visible at Γ while one finds a broad structure at the corner of the Brillouin zone. The SCBA reproduces the peak in the spectrum at Γ; however, its position is shifted to higher energies. At K, the SCBA spectrum shows a structure which becomes broader when the system size is increased from $N_s = 21$ to $N_s = 36 \times 36$ (dotted lines). On the other hand, in all cases where we find a quasiparticle peak, the SCBA results for $N_s = 21$ and for $N_s = 36 \times 36$ are indistinguishable. Thus we conclude that for $t = 1$ the quasiparticle peak disappears if one changes the wavevector from the Γ point to the corner of the Brillouin zone, *cf.* Figure 1. While there remain differences, we find that overall the SCBA reproduces the qualitative features of the exact results.

Finally we discuss the energy dispersion of one hole. We define the dispersion as the difference of the position of the maximum of $A(\mathbf{k}, \omega)$ for a given $\mathbf{k}$ and the one hole creation energy $E_{1,loc}^{SCBA}$ (see Tab. 1), *i.e.* the position

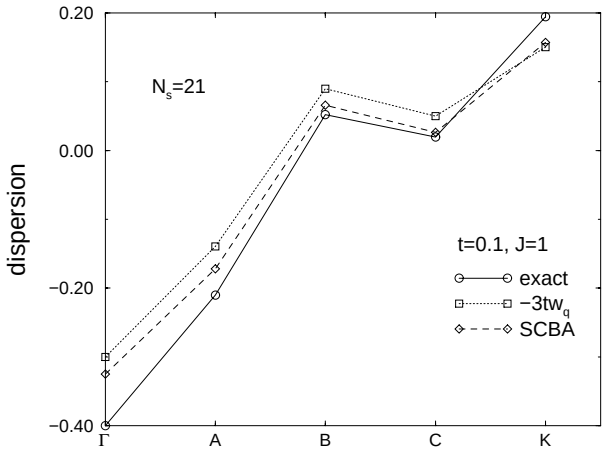

Fig. 4. The dispersion of one hole as defined in the text for $t = 0.1$, $J = 1$ and $N_s = 21$ sites. The symbols ($\circ$) show the exact results, the diamonds ($\diamond$) the results of the SCBA and the squares ($\square$) the lowest order approximation for the Green's function.

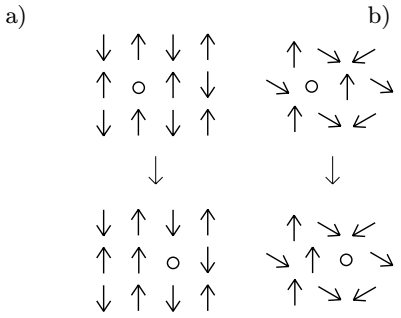

Fig. 5. Spin arrangement of $|\Phi_{\mathbf{r}}\rangle$ (top) and $c_{\mathbf{r}+\boldsymbol{\delta}\uparrow}c^{\dagger}_{\mathbf{r}\uparrow}|\Phi_{\mathbf{r}}\rangle$ (bottom) for (a) the square lattice AF and (b) the triangular AF.

of the maximum for $t = 0$. In Figure 4, we show the dispersion for $N_s = 21$ sites for $t = 0.1$ and $J = 1$. The circles (connected by solid lines) show the results of the exact diagonalization. They follow closely the free dispersion of the hole, $\epsilon_{\mathbf{q}} - 3J/4 = -3\,t\,w_{\mathbf{q}}$ (shown as boxes). The SCBA (diamonds) yields an improvement towards the exact results for all points of the Brillouin zone. Obviously, the free dispersion is already a good approximation of the exact results.

5 Summary

In this work, we have developed a formalism which allows the derivation of effective Hamiltonians for the motion of holes in an arbitrarily ordered spin background. Fundamental to this development was the construction of a coherent state approximation for the electron states, which automatically excludes double occupancy. In this representation, the partition function of an arbitrary number of holes can be cast into the form of a path integral which still contains the full non-linear coupling of the holes to the spin degrees of freedom of the background. As a first application of this formalism, we have rederived the well known effective Hamiltonian $\mathcal{H}_{\square}$ for the motion of a single hole in the collinear antiferromagnetic order of the square lattice antiferromagnet in the linear spin wave approximation. The derivation of the effective Hamiltonian $\mathcal{H}_{\triangle}$ of a single hole moving in the planar spin arrangement of the triangular antiferromagnet also makes use of the linear spin wave approximation. However, in this case, special care has to be taken to ensure a proper treatment of the Goldstone modes which must not couple to the hole [20]. In contrast to the square lattice AF, where hopping of the hole from a lattice site $\mathbf{r}$ to a neighbouring site $\mathbf{r}+\boldsymbol{\delta}$ is necessarily accompanied by a *spin flip* at site $\mathbf{r}$, the same hopping process requires only a *rotation of the spin* at $\mathbf{r}$ by $\pm$ 120° in the case of the triangular AF, see Figure 5.

In other words, if $|\Phi^{(0)}_{\mathbf{r}}\rangle$ is the groundstate with one hole at $\mathbf{r}$ in the undistorted spin background of the AFs, then the hopping matrix element $\langle\Phi^{(0)}_{\mathbf{r}+\boldsymbol{\delta}}|c_{\mathbf{r}+\boldsymbol{\delta}\sigma}c^{\dagger}_{\mathbf{r}\sigma}|\Phi^{(0)}_{\mathbf{r}}\rangle$ is always zero for the square lattice AF, while it is $+1/2$ for the triangular AF. This accounts for the main difference between the hole dynamics in the collinear square lattice AF and the planar triangular AF.

On the square lattice, the hole can hop due to the zero point fluctuations of the AF background. In this case, magnon-assisted hopping happens predominantly between the sites of the same magnetic sublattice. This leads to a minimum of the hole dispersion at a quarter of a reciprocal lattice vector of the square lattice. By contrast, on the triangular lattice, hole hopping between nearest neighbour sites, *i.e.* between different magnetic sublattices, is also possible without magnon assistance. Thus, for $J \gg t$, where magnon assisted processes are energetically suppressed, the hole dispersion in the triangular AF will be dominated by the bare (unassisted) hopping processes. This has been confirmed by comparing the exact dispersion of the bare hole in the 21 site sample for $t = 0.1J$. The approximate inclusion of the magnon-assisted processes in the calculation of the dispersion by the self-consistent Born approximation has been found to improve the agreement with the exact dispersion. The exact one-hole Lagrangian (10-12), evaluated in spin wave approximation, leads to results in reasonable agreement with exact numerical diagonalization of small systems. $\mathcal{L}$ provides thus a firm basis for a derivation of a continuum model which is capable of describing the full non-linearities of the spin fields in the presence of single holes.

Note added in proof

After completion of this work, we became aware of the derivation of an effective Hamiltonian for the motion of holes on the triangular lattice in reference [20]. The effective Hamiltonian there differs significantly from our result (15), since the problem arising form the coupling of the hole motion to the Goldstone modes has been ignored in [20].

Appendix

A straightforward expansion of $\mathcal{L}$ around the classically ordered state with respect to the fields θ and ϕ, and a subsequent integration of ψ leads to the appearance of zero energy spin wave amplitudes in linear order in the hopping term $\mathcal{L}_t$. This is in contradiction to the spin rotational invariance of the model (1). In order to resolve the contradiction, we now verify that this invariance persists in an appropriate spin wave expansion. In the first order expansion around the state given by $\phi_{\mathbf{r}} = \phi^{(0)}_{\mathbf{r}}$, $\theta_{\mathbf{r}} = \pi/2$ (*cf.* Eq. (13)), the critical term $\mathcal{L}_t$ reads

$$\mathcal{L}_t = -t \sum_{\langle \mathbf{r},\mathbf{r}'\rangle} \Big\{ \eta^*_{\mathbf{r}'}\eta_{\mathbf{r}}\, e^{-\frac{i}{2}(\psi_{\mathbf{r}'}-\psi_{\mathbf{r}})} \times \left[\cos\left(\frac{\phi^{(0)}_{\mathbf{r}} - \phi^{(0)}_{\mathbf{r}'}}{2}\right) - \sin\left(\frac{\phi^{(0)}_{\mathbf{r}} - \phi^{(0)}_{\mathbf{r}'}}{2}\right) \times \left(i\frac{p_{\mathbf{r}} + p_{\mathbf{r}'}}{\sqrt{2}} + \frac{x_{\mathbf{r}} - x_{\mathbf{r}'}}{\sqrt{2}}\right)\right] + \quad \mathbf{r} \leftrightarrow \mathbf{r}' \Big\}\cdot \quad \text{(A.1)}$$

This expression is valid for both the square, and the triangular lattice. We now perform an infinitesimal homogeneous rotation in spin space parametrized by the angles

$\boldsymbol{\epsilon}$. The corresponding transformation of the fields can be read off from (2). The field η is unchanged and the linear changes in ψ, θ, and ϕ are (we express the last two fields by x and p)

$$\begin{aligned}\psi'_{\mathbf{r}} &= \psi_{\mathbf{r}} + 2\left[\epsilon^x \cos\phi^{(0)}_{\mathbf{r}} + \epsilon^y \sin\phi^{(0)}_{\mathbf{r}}\right]\\ x'_{\mathbf{r}} &= x_{\mathbf{r}} + \sqrt{2}\epsilon^z\\ p'_{\mathbf{r}} &= p_{\mathbf{r}} + \sqrt{2}\left[-\epsilon^x \sin\phi^{(0)}_{\mathbf{r}} + \epsilon^y \cos\phi^{(0)}_{\mathbf{r}}\right]. \end{aligned} \quad \text{(A.2)}$$

Substituting these rotated fields for the original ones in (A.1), one sees that ϵ^z drops out and the change in the field $p_{\mathbf{r}}$ induced by the other two rotations ϵ^x and ϵ^y is compensated by the corresponding change in the field $\psi_{\mathbf{r}}$. Thus, we see that $\mathcal{L}_t$, and hence the whole Lagrangian, is invariant under an infinitesimal rotation in spin space as it should be. It is only after the integration over the field ψ that the invariance appears to be lost.

Turning to the case of the square lattice, where $\phi^{(0)}_{\mathbf{r}} = \pm\,\pi/2$ ($\cos\phi^{(0)}_{\mathbf{r}} = 0$), the zero modes are seen to decouple in $\psi_{\mathbf{r}}$ and $p_{\mathbf{r}}$ (*cf.* (A.2)), and in $\mathcal{L}_t$ the term of zeroth order in the fields $x_{\mathbf{r}}$ and $p_{\mathbf{r}}$ vanishes. It is easily verified from the spin wave expansion of $\mathcal{L}_J$ that the zero modes are given by $x_{\mathbf{r}} = x$, $p_{\mathbf{r}} = 0$ and $x_{\mathbf{r}} = 0$, $p_{\mathbf{r}} = p\sin\phi^{(0)}_{\mathbf{r}}$ which both cancel in $\mathcal{L}_t$. After substituting $\eta\, e^{\frac{i}{2}(\psi-\phi^{(0)})}$ by h, we can integrate over ψ, and return to the operator form. Thus, the spin wave expansion as sketched in the main text leads to the correct result [15].

In the case of the triangular lattice, where $\phi^{(0)}_{\mathbf{r}} = 2\pi/3, 0, -2\pi/3$ for the three sublattices respectively, the zero modes in $\psi_{\mathbf{r}}$ and $p_{\mathbf{r}}$ mix. Again, it is easily verified from the spin wave expansion of $\mathcal{L}_J$ that they are given by $x_{\mathbf{r}} = x$, $p_{\mathbf{r}} = 0$, and $x_{\mathbf{r}} = 0$, $p_{\mathbf{r}} = p\sin\phi^{(0)}_{\mathbf{r}}$, and $x_{\mathbf{r}} = 0$, $p_{\mathbf{r}} = p\cos\phi^{(0)}_{\mathbf{r}}$. The first mode cancels in $\mathcal{L}_t$, but the last two remain, if one disregards ψ. However, we are free to apply a canonical transformation to the fields ψ, x, and p in the path integral. We choose

$$\begin{aligned}\psi_{\mathbf{r}} &\to \psi_{\mathbf{r}} + \sqrt{\frac{2}{3}}\Big(p_{\mathbf{r}} + \frac{2}{3}\sum_{j=1}^{3} p_{\mathbf{r}+\boldsymbol{\delta}_j}\Big)\\ x_{\mathbf{r}} &\to x_{\mathbf{r}} + \sqrt{\frac{1}{6}}\Big(\eta^*_{\mathbf{r}}\eta_{\mathbf{r}} + \frac{2}{3}\sum_{j=1}^{3}\eta^*_{\mathbf{r}-\boldsymbol{\delta}_j}\eta_{\mathbf{r}-\boldsymbol{\delta}_j}\Big)\\ p_{\mathbf{r}} &\to p_{\mathbf{r}}. \end{aligned} \quad \text{(A.3)}$$

($\boldsymbol{\delta}_j = (\cos\varphi_j, \sin\varphi_j)$, $\varphi_j = \frac{2\pi}{3}j$ are three of the six nearest neighbour vectors.) With this choice (i) the new field ψ remains invariant under homogeneous rotations in spin space, *i.e.* it does not contain a zero mode, and (ii) $\mathcal{L}_{kin}$ is changed only by a total time derivative which yields no change in the action (the latter condition is equivalent to the transformation being canonical). After applying (A.3) to $\mathcal{L}$, all zero modes cancel in $\mathcal{L}_t$. We substitute $\eta\, e^{\frac{i}{2}(\psi-3\phi^{(0)})}$ by h, integrate over ψ, and return to the operator representation. The result for $\mathcal{H}_\triangle$ is the expression (15).

References

1. E. Dagotto, Rev. Mod. Phys. **66**, 763 (1994).
2. T. Tohyama, S. Maekawa, J. Phys. Soc. Jpn **65**, 1902 (1996).
3. T. Xiang, J.M. Wheatley, Phys. Rev. B **54**, 12653 (1996).
4. R. Hayn, A.F. Barabanov, J. Schulenburg, J. Richter, Phys. Rev. B **53**, 11714 (1996).
5. D.N. Sheng, Y.C. Chen, Z.Y. Weng, Phys. Rev. Lett. **77**, 5102 (1996).
6. M. Vojta, K.W. Becker, Phys. Rev. B **54**, 15483 (1996).
7. W.F. Brinkman, T.M. Rice, Phys. Rev. B **2**, 1324 (1970).
8. S.A. Trugman, Phys. Rev. B **42**, 6612 (1990).
9. T. Li, P. Wölfle, P.J. Hirschfeld, Phys. Rev. B **40**, 6817 (1989).
10. U. Pecher, H. Büttner, Z. Phys. B Cond. Matter **98**, 239 (1995).
11. A. Auerbach, B.E. Larson, Phys. Rev. Lett. **66**, 2262 (1991).
12. R. Shankar, Phys. Rev. Lett. **63**, 203 (1989); Nucl. Phys. B **330**, 433 (1990).
13. P.B. Wiegmann, Phys. Rev. Lett. **60**, 821 (1988).
14. C.L. Kane, P.A. Lee, N. Read, Phys. Rev. B **39**, 6880 (1989).
15. F. Marsiglio, A.E. Ruckenstein, S. Schmitt-Rink, C.M. Varma, Phys. Rev. B **43**, 10882 (1991).
16. H. Barentzen, P. Wróbel, Z. Phys. B Cond. Matter **93**, 375 (1994).
17. We thank A.H. MacDonald for a discussion of this point.
18. B. Bernu, P. Lecheminant, C. Lhuillier, L. Pierre, Phys. Rev. B **50**, 10048 (1994).
19. R. Haydock, V. Heine, M.J. Kelly, J. Phys. C **5**, 2845 (1972).
20. M. Azzouz, T. Dombre, Phys. Rev. B **53**, 402 (1996).